Hydrothermal Synthesis and Characterization of Uranium-Containing MCM-48 Samples

Dharmesh Kumar,[†] K. T. Pillai,[‡] V. Sudersanan,[§] G. K. Dey,[||] and N. M. Gupta*,[†]

Divisions of Applied Chemistry, Fuel Chemistry, Novel Materials and Structural Chemistry, and Materials Science, Bhabha Atomic Research Centre, Trombay, Mumbai 400 085, India

Received April 1, 2003. Revised Manuscript Received July 11, 2003

MCM-48 samples containing uranium (U−MCM-48) to the extent of 1 to 6 wt % were synthesized hydrothermally and characterized using powder XRD, ^{29}Si MAS NMR, FTIR spectroscopy, DR UV−Vis spectroscopy, N_2 sorption, and TEM techniques. These analyses confirmed the formation of an ordered cubic-phase MCM-48 mesomaterial where the uranium existed in the hexavalent state forming a local uranate type structure. A part of the uranyl groups were found to be incorporated in the framework positions, while the rest were anchored on to the wall of the host silica matrix. Also, the U−MCM-48 samples exhibited an enlargement of the cubic cell unit as well as an increase in the degree of cross-linking, as revealed by XRD and MAS NMR results. The samples exhibited N_2 sorption isotherms of type IV and an increase was observed in the pore diameter as a result of uranium incorporation. TEM investigation revealed that although U−MCM-48 samples were of cubic symmetry similar to that of Si−MCM-48, some distortion in the pore structure was clearly noticeable. Furthermore, in case of the samples with U loading of ∼6 wt %, formation of nanocrystallites of α-U_3O_8 was also detected after calcination and such samples consisted of a multiple-size pore system.

Introduction

A number of substitutions have been attempted at the framework silicon sites of mesoporous molecular sieves, particularly in the case of MCM-41 having a hexagonal uni-dimensional pore structure and in MCM-48 displaying a three-dimensional cubic structure. The list of the substituents is fairly large, some of them being Al,[1,2] Ti,[3−5] V,[3,6−8] Cr,[3,7,9] Fe,[2,10] Mn,[11] and Ga.[2] The objective of such substitutions has been to engineer the pore structure and the texture of these wide-pore materials so that they may serve as hosts to guest molecules of the desired size.[12,13] This, over all, helps in developing a tailor-made catalyst system that may exhibit the requisite activity and selectivity. Some of the recent publications have advocated the use of lanthanides or actinides as substituents and it is suggested that their higher electrophilic character may result in a better catalytic performance.[14,15] The incorporation of uranium into mesoporous hosts, silicates, zeolites, and clays etc. is therefore of considerable interest, both because of the potential use in catalysis and also for possible application in the area of nuclear waste management.[16,17] We demonstrated recently that the oxides of uranium may be anchored in the channels of MCM-41 and MCM-48 molecular sieves, and these materials exhibit unique catalytic properties for oxidation of CO and CH_3OH, depending on the oxidation state and the size of uranium oxide crystallites.[18−21] It has also been demonstrated that a larger amount of uranium could be loaded into MCM-48, as compared to MCM-41, because of its three-dimensional cubic pore system.[18] In continuation of these previous studies, we have now attempted uranium incorporation in the framework of siliceous

* To whom correspondence should be addressed. Fax: 091-22-25505151 or 25519613. E-mail: nmgupta@magnum.barc.ernet.in.
[†] Applied Chemistry Division.
[‡] Fuel Chemistry Division.
[§] Novel Materials and Structural Chemistry Division.
[||] Materials Science Division.

(1) Romero, A. A.; Alba, M. D.; Klinowski, J. *J. Phys. Chem. B* **1998**, *102*, 123.
(2) Kosslick, H.; Lischke, G.; Landmesser, H.; Parlitz, B.; Storek, W.; Fricke, R. *J. Catal.* **1998**, *176*, 102.
(3) Zhang, W.; Pinnavaia, T. J. *Catal. Lett.* **1996**, *38*, 261.
(4) Koyano, K. A.; Tatsumi, T. *Chem. Commun.* **1996**, 145.
(5) Zhang, W.; Froba, M.; Wang, J.; Tanev, P. T.; Wong, J.; Pinnavaia, T. *J. Am. Chem. Soc.* **1996**, *118*, 9164.
(6) Luan, Z.; Xu, J.; He, H.; Klinowski, J.; Kevan, L. *J. Phys. Chem. B* **1996**, *100*, 19595.
(7) Yuan, Z. Y.; Wang, J. Z.; Zhang, Z. L.; Chen, T. H.; Li, H. X. *Microporous Mesoporous Mater.* **2001**, *43*, 227.
(8) Reddy, K. M.; Moudrakovski, I.; Sayari, A. *J. Chem. Soc., Chem. Commun.* **1994**, 1059.
(9) Zhu, Z.; Chang, Z.; Kevan, L. *J. Phys. Chem. B* **1999**, *103*, 2680.
(10) Zhao, W.; Luo, Y.; Deng, P.; Li, Q. *Catal. Lett.* **2001**, *73*, 199.
(11) Zhao, D.; Goldfarb, D.; *J. Chem. Soc., Chem. Commun.* **1995**, 875.
(12) Corma, A. *Chem. Rev.* **1997**, *97*, 2373.
(13) Biz, S.; Occelli, M. L. *Catal. Rev. Sci. Eng.* **1998**, *40*, 329.
(14) Tismaneanu, R.; Ray, B.; Khalfin, R.; Semiat, R.; Eisen, M. S. *J. Mol. Catal. A: Chem.* **2001**, *171*, 229.
(15) Lam, D. J.; Veal, B. W.; Paulikas, A. P. *ACS Symp. Ser.* **1983**, *216*, 145.
(16) Suib, S. L.; Kostapapas, A.; Psaras, D. *J. Am. Chem. Soc.* **1984**, *106*, 1614.
(17) Zhang, Z. T.; Konduru, M.; Dai, S.; Overbury, S. H. *Chem. Commun.* **2002**, 2406.
(18) Vidya, K.; Dapurkar, S. E.; Selvam, P.; Badamali, S. K.; Gupta, N. M. *Microporous Mesoporous Mater.* **2001**, *50*, 173.
(19) Vidya, K.; Dapurkar, S. E.; Selvam, P.; Badamali, S. K.; Kumar, D.; Gupta, N. M. *J. Mol. Catal. A: Chem.* **2002**, *181*, 91.
(20) Kumar, D.; Kamble, V. S.; Gupta, N. M.; *Catal. Lett.* **2003**, *88*, 175.
(21) Kumar, D.; Vidya, K.; Selvam, P.; Dey, G. K.; Gupta, N. M. *Advances in Nanosciences and Nanotechnology*; Niscom: Delhi (in press).

10.1021/cm030269s CCC: $25.00
Published on Web 08/26/2003

MCM-48 material. A conventional hydrothermal synthesis procedure has been adopted for this purpose. For the sake of comparison, a typical MCM-48 sample consisting of a similar amount of uranium was prepared by a wet impregnation route, to enable us to establish the influence of preparation condition on the location of the incorporated uranium. The samples were characterized using X-ray diffraction, ^{29}Si MAS NMR, FTIR spectroscopy, DR−UV−visible spectroscopy, physical adsorption of N_2, and TEM techniques. The results of these studies are presented in this article.

Experimental Section

Synthesis. The siliceous MCM-48 (referred to as Si−MCM-48) and corresponding uranium containing MCM-48 material (referred to as U−MCM-48) were synthesized utilizing tetra ethyl orthorsilicate (TEOS) (Merck) as silicon source, *n*-cetyl trimethylammonium bromide (CTAB) (Lancaster) as surfactant, NaOH (S. D. Fine Chem.) as a base, and uranyl actetate monohydrate (Merck) as uranium metal precursor.

As a first step, a gel of molar composition of TEOS/CTAB/NaOH/UO_2/H_2O (1:0.62:0.48:0−0.0036:61) was prepared with continuous stirring. The pH was adjusted to about 11, and after further stirring for about 1 h the resulting gel was charged into a Teflon-lined autoclave. After heating at 383 K for 8 days, the solid product was filtered and washed thoroughly with distilled water, followed by oven-drying at 353 K. These are designated as as-synthesized samples in the text. The samples were finally calcined in a tubular furnace at 823 K, first in a flow of N_2 (60 mL/min) for 1 h and then in O_2 (60 mL/min) for 8 h, at a heating rate of 2 °C/min. The calcined samples were analyzed for U by spectrophotometry and are designated as U−MCM-48A, U−MCM-48B, and U−MCM-48C, where A, B, and C refer to the samples with uranium content of about 1, 3, and 6 wt %, respectively.

For preparing a sample by impregnation route, 1.0 g of template free MCM-48 was contacted with 0.06 molar aqueous solution of uranyl acetate under continuous stirring. The sample was washed thoroughly with distilled water, dried at room temperature, and then calcined at 823 K as in the case of U−MCM-48 samples. The uranium content of the sample, designated as IU−MCM-48, was ∼8 wt %.

Sample Characterization. *Powder X-ray Diffraction (XRD).* XRD patterns of the samples were recorded in the 2θ region of 2−10° on a Philips analytical diffractometer using nickel-filtered Cu Kα radiation (λ = 1.54056 Å). The scan speed and the step size were 0.2°/min and 0.02°, respectively. The XRD patterns were also recorded in the region of 10−60° to monitor the formation of bulk oxides of uranium, if any.

Magic-Angle-Spinning (MAS) NMR. The solid-state ^{29}Si MAS NMR spectra were measured on a Bruker model DPX-300 spectrometer at a resonance frequency of 59.6 MHz. The powdered samples were placed in 7.0-mm-diam. zirconia rotors and spun at a rate of 5.0 kHz. The chemical shifts were determined using tetraethyl orthosilicate (δ = −82.4 ppm from TMS) as the reference compound.

Fourier Transform Infrared Spectroscopy (FTIR). A Jasco-610 spectrophotometer was employed to record the FTIR spectra in mid-IR region (4000−400 cm^{-1}) and at a resolution of 4 cm^{-1}. Compressed KBr pellets containing about 5 wt % of a sample were used for this purpose. Each spectrum was collected on co-adding of 100 scans.

Diffuse Reflectance−Ultraviolet−Visible (DR−UV−Visible) Spectroscopy. DR−UV−Visible spectra were recorded on a Shimadzu UV-260 spectrophotometer. The powder samples were loaded between quartz windows and the spectra were collected in the 250−600-nm wavelength range using $BaSO_4$ as a reference.

Nitrogen Sorption. The physical adsorption−desorption isotherms of nitrogen were monitored at 77 K with a Sorptomatic model 1990 instrument. The samples were dehydrated under vacuum at 373 K for 1 h and then degassed (523 K) overnight prior to analyses. The BET surface area and the pore size distribution were determined with the help of these data.

Transmission Electron Microscopy (TEM). The TEM studies were carried out using a JEOL 2000 FX instrument operating at 120 kV. The samples for analysis were prepared by ultrasonicating 300-mesh-size material in ethanol and then dispersing on a carbon film supported on copper grid.

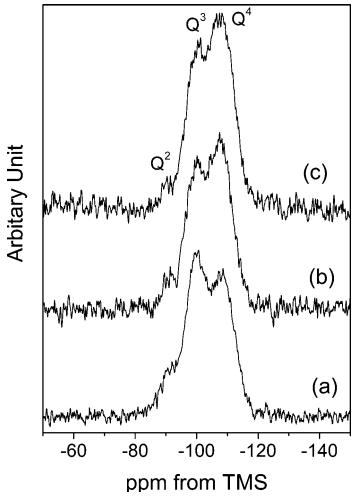

Figure 1. ^{29}Si MAS NMR spectra of (a) Si−MCM-48, (b) U−MCM-48B, and (c) U−MCM-48C.

Results and Discussion

^{29}Si MAS NMR. The representative ^{29}Si MAS NMR spectra of Si−MCM-48 and U−MCM-48 samples are presented in Figure 1. All the samples exhibited a three-line pattern with the mean chemical shift (δ) values of about −91.3, −99.2, and −107.8 ppm. They are assigned to $(SiO)_2-Si(OH)_2$ (Q^2), $(SiO)_3-SiOH$ (Q^3), and $Si(SiO)_4$ (Q^4 sites or groups), respectively.[22,23] A significant increase is observed in the Q^4-sites for the U−MCM-48 samples, with the Q^4/Q^3 intensity ratio increasing to a value of ∼1.2 in the NMR spectrum of Figure 1c as compared to a corresponding value of ∼0.7 in the case of Figure 1a for a U-free MCM-48 sample. We also observe in Figure 1b and c a progressive broadening of the Q^4 signal as a result of uranium incorporation. These features are akin to those reported earlier for incorporation and substitution of transition metals into the silicate framework of mesoporous materials.[3,6] Thus, as discussed in ref 3, the increase in the width and intensity of the Q^4 line along with the simultaneous decrease in intensity of Q^2 and Q^3 NMR signals in spectra (b) and (c) of Figure 1 are indicative of substitution of uranium at the silicate framework resulting thereby in the promotion of the cross linking of silicate defect sites (Q^2 and Q^3). This in turn would lead to the increased number of Si sites with four bridging oxygen neighbors, and hence to the increase of the thickness of mesoporous walls of MCM-48 silicate matrix. Such a process of uranium induced polymerization of silica moieties has indeed been reported in previous studies.[24,25]

(22) Huo, Q.; Margolese, D. I.; Stucky, G. D. *Chem. Mater.* **1996**, *8*, 1147.
(23) Xu, J.; Luan, Z.; He, H.; Zhou, W.; Kevan, L. *Chem. Mater.* **1998**, *10*, 3690.

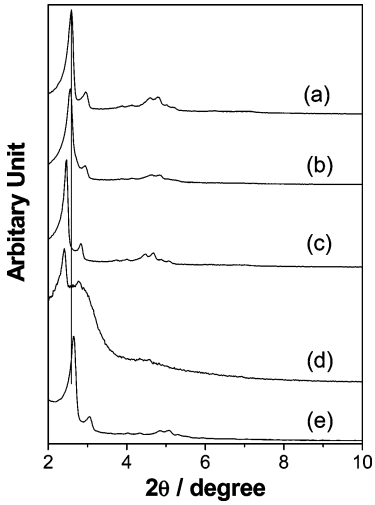

Figure 2. Low-Angle XRD patterns of (a) Si−MCM-48, (b) U−MCM-48A, (c) U−MCM-48B, (d) U−MCM-48C, and (e) IU−MCM-48.

Table 1. XRD Parameters of Si−MCM-48 and U−MCM-48 Samples: *d* Values of Reflections and Constants of the Unit Cell

sample	d{*hkl*}/Å		unit cell parameter (a_0/Å)[a]
	211	220	
Si−MCM-48	34.34	29.81	84.22
U−MCM-48A	34.51	30.10	84.83
U−MCM-48B	35.79	31.07	87.77
U−MCM-48C	36.57	31.57	89.50
IU−MCM-48	33.04	28.72	81.06

[a] $a_0 = d\ \{hkl\}\ \sqrt{h^2+k^2+l^2}$

XRD. Figure 2 depicts the powder X-ray diffraction patterns in the 2θ region of 2 to 10° for Si−MCM-48 (curve a), U−MCM-48 samples with different uranium loadings (curves b−d), and the IU−MCM-48 sample synthesized through impregnation route (curve e). The *hkl* index corresponding to the reflections in Figure 2a are found to be in good agreement with those reported for the cubic Si−MCM-48 material and the *d* spacings are compatible with the cubic *Ia*3*d* space group.[22,23,26−28] The most intense {211} XRD line of Si−MCM-48 appears at 2θ ∼2.6° along with a distinct shoulder at 2θ ∼3.0°, representing the {220} reflection. Also, other low intensity reflections of higher order appear in the 2θ region of 3 to 6°, which is a well-documented feature of MCM-48. In the case of U−MCM-48 samples, these main reflections are found to shift to marginally lower 2θ values (Figure 2 b−d). Thus, in the case of U−MCM-48C sample containing 6 wt % uranium (Figure 2d), the {211} and {220} lines appear at 2θ values of 2.4° and 2.78°, respectively. The variation in the *d* values corresponding to these reflections as a function of U-loading and the values of the cubic unit cell constant (a_o) of different calcined samples are given in Table 1. As can be seen in these data, the value of the unit cell constant

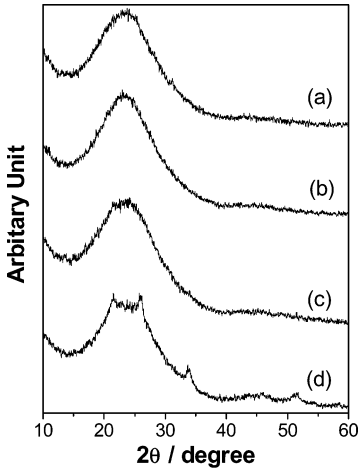

Figure 3. High-Angle XRD patterns of (a) Si−MCM-48, (b) U−MCM-48A, (c) U−MCM-48B, and (d) U−MCM-48C.

(a_o) increases progressively with the increasing loading of uranium. Similar changes in the *d* values and in the unit cell parameter have been reported earlier for incorporation and/or substitution of other metal ions or radicals into the silicate framework.[2,3,29] As has been discussed in ref 8, the insertion of a heteroatom metal radical such as U−O with larger M−O bond distance of ∼2.3 Å,[24] in place of Si−O (∼1.65 Å), may lead to an increase in the unit cell parameter. Another process that may account for an increase in the unit cell parameter is the increase in the wall thickness of MCM-48 because of uranium incorporation, the happening of which is revealed by the NMR results described above. The XRD results thus confirm that a part of uranium gets incorporated into the framework positions of the silica network of MCM-48. In U−MCM-48C a significant decrease is observed in the intensity of the forementioned XRD reflections and additional weak reflections are also noticed in the 2θ region between 2.5 and 3° (Figure 2d). In contrast to the observations reported above, a decrease was observed in the *d* values and also in the unit cell parameter in the IU−MCM-48 sample (Figure 2e). Such a change is generally attributed to an increase in the destructive interferences arising due to the filling of pores. In general, it is reported that the introduction of a scattering material into the pores leads to an increased phase cancellation between scattering from the wall and the pore regions and therefore to the reduced scattering intensities of Bragg reflections. Such a phenomenon has been reported for other metal oxide systems within the pores of a mesoporous silicate matrix.[30,31]

The XRD patterns recorded in the 2θ region of 10−60° for U−MCM-48 and Si−MCM-48 samples are shown in Figure 3. The weak reflections observed at *d* values of 4.15, 3.39, 2.62, 2.07, 1.96, and 1.75 Å in U−MCM-48C (curve d) are indexed to α-U_3O_8 (JCP Card no. 24-1172). These results thus indicate that for the loadings of ∼6 wt % and above a part of uranium may exist as a secondary phase comprising α-U_3O_8. The

(24) Reich, T.; Moll, H.; Denecke, M. A.; Geipel, G.; Bernhard, G.; Nitsche, H.; Allen, P. G.; Bucher, J. J.; Kaltsoyannis, N.; Edelstein, N. M.; Shuh, D. D. *Radiochim. Acta* **1996**, *74*, 219.
(25) Hrnecek, E.; Irlweck, K. *Radiochim. Acta* **1999**, *87*, 29.
(26) Kresge, C.T.; Leonowicz, M. E.; Roth, W. J.; Vartuli, J. C.; Beck, J. S. *Nature* **1992**, *359*, 710.
(27) Fyfe, C. A.; Fu, G. *J. Am. Chem. Soc.* **1995**, *117*, 9709.
(28) Romero, A. A.; Alba, M. D.; Zhou, W.; Klinowski, J. *J. Phys. Chem. B* **1997**, *101*, 5294.
(29) Laha, S. C.; Mukherjee, P.; Sainkar, S. R.; Kumar, R. *J. Catal.* **2002**, *207*, 213.
(30) Lim, M. H.; Blanford, C. F.; Stein, A. *Chem. Mater.* **1998**, *10*, 467.
(31) Fröba, M.; Köhn, R.; Bouffaud, G. *Chem. Mater.* **1999**, *11*, 2858.

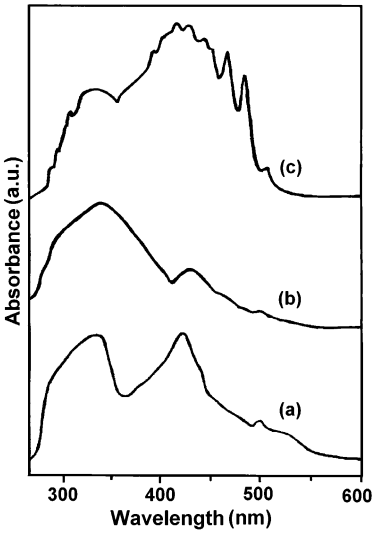

Figure 4. DR UV−Vis spectra of (a) as-synthesized U−MCM-48C, (b) U−MCM-48C, and (c) uranyl acetate monohydrate.

average size of these crystallites of uranium oxide is found to be ~3.7 nm, as estimated from XRD data using the Debye−Scherrer equation. The broad feature in the XRD patterns of curves a−c in Figure 3 is due to the widely reported noncrystalline component of silica framework.[32,33]

DR UV−Visible Spectroscopy. The DR UV−Visible spectra of as-synthesized and calcined U−MCM-48C samples are presented by curves a and b, respectively, in Figure 4. For comparison, the spectrum of uranyl acetate is included in curve c, which shows the characteristic structure due to the electron-vibration interaction, typical of a UO_2^{2+} moiety.[33−36] The absorption spectrum of uranyl ion consists of 14 transitions in the 300−600 nm region, where each band overlaps the adjacent band on both the high and low-frequency side of the band center resulting thereby in rather ill-defined and overlapping spectra.[34−36] It is also reported that the individual transitions are affected by various parameters such as changes in ligand, temperature, and medium, etc.[34−36] A comparison of spectra in Figure 4 thus reveals that uranium exists in a hexavalent state, i.e., in the form of uranyl species (UO_2^{2+}), in the as-synthesized U−MCM-48 sample. In the U−MCM-48C sample (Figure 4b), not only are the absorbance bands broader, we also observe strong absorbance in the 300−375 nm region while at the same time the intensity of the 350−450 nm region band (cf. Figure 4a) decreased drastically. These features could be attributed to the perturbations arising due to bonding of O═U═O units to ≡Si−O− units, thus forming a local uranate type structure.[14] Also, a decrease in the intensity of the 350−450 nm band in Figure 4b indicates a decrease in the concentration of uranyl groups upon calcination. This may be ascribed to conversion of some of the uranyl moieties to α-U_3O_8, as is evident from XRD data of Figure 3d as well.

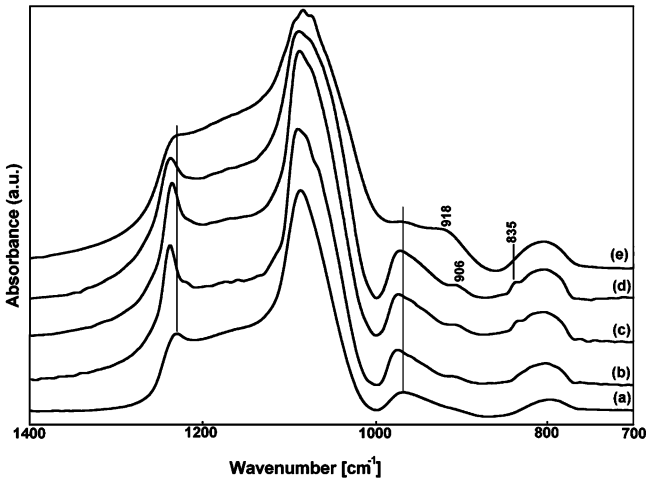

Figure 5. FTIR spectra of (a) Si−MCM-48, (b) U−MCM-48A, (c) U−MCM-48B, (d) U−MCM-48C, and (e) IU−MCM-48.

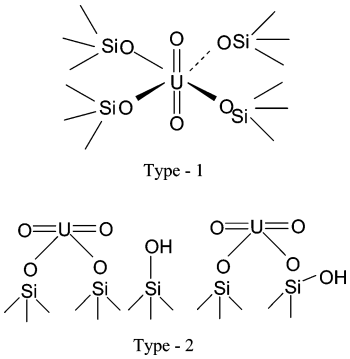

Figure 6. Schematic pictures of two alternative modes of uranium incorporation into the framework of MCM-41 during hydrothermal synthesis: Type 1, incorporation of uranium in the framework sites of silica matrix; and Type 2, uranyl groups bonded at the terminal sites of mesoporous wall of MCM-48.

FTIR Study. Figure 5 depicts the IR spectra in the framework region of Si−MCM-48 (curve a), and U−MCM-48 samples (curves b−d). The IR spectrum of a IU−MCM-48 sample prepared by impregnation route is also included in this figure (curve e) for comparison. The vibrational bands at 1230 and 1084 cm^{-1} are typical of Si−MCM-48 samples and arise due to ν_{as}(Si−O−Si) vibrations of the silica framework. The 800 cm^{-1} band in this figure is due to the corresponding ν_s(Si−O−Si) stretching vibrations.[1,6,28,29] These framework vibrations experience a blue shift of ca. 3−5 cm^{-1} in their frequency in U−MCM-48 samples (Figure 5 b−d), indicating a definite perturbation of the framework. In addition, we also observe the development of shoulder bands at about 1064 cm^{-1} in the spectra b−d of Figure 5, the intensity of which increased with increase in U loading. These bands may be ascribed to the stretching vibrations of (Si−O−U) groups indicating again the binding of the uranium at silica sites. Also of interest is the blue shift in the 970 cm^{-1} band in Figure 5a, which is normally attributed to terminal Si−O^-H^+ groups of a calcined MCM-48 sample.[1,6,28,29] The intensity of this band, appearing at 974 cm^{-1} in Figures 5 b−d, increases progressively with the increasing uranium content. This change in IR spectra is therefore attributed to the linkages of uranyl groups at the terminal silica sites of MCM-48 walls.

(32) Zhang, W.-H.; Shi, J.-J.; Wang, L.-Z.; Yan, D.-S. *Chem. Mater.* **2000**, *12*, 1408.
(33) Iwamoto, M.; Abe, T.; Tachibana, Y. *J. Mol. Catal. A: Chem.* **2000**, *155*, 143.
(34) McGlynn, S. P.; Smith, J. K. *J. Mol. Spectrosc.* **1961**, *6*, 164.
(35) Jeżowska-Trzebiatowska, B.; Bartecki, A. *Spectrochim. Acta* **1962**, *18*, 799.

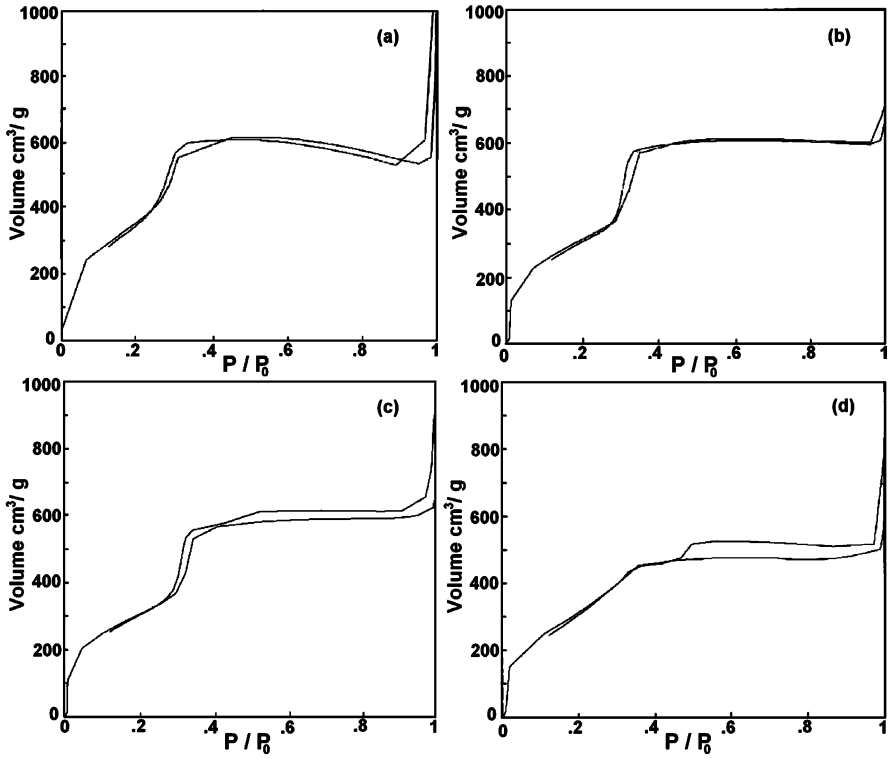

Figure 7. Nitrogen sorption isotherms of (a) Si−MCM-48, (b) U−MCM-48A, (c) U−MCM-48B, and (d) U−MCM-48C.

In the case of U−MCM-48 samples (curves b−d), we also notice additional IR bands at 906 and 835 cm^{-1} due to asymmetric and symmetric stretching vibrations of uranyl species.[37] It is known that these bands appear at ∼930 and 856 cm^{-1}, respectively, in the case of uranyl acetate.[38] It is well documented that U═O stretching frequency in uranyl compounds changes with change of the ligand and a relationship exists between this frequency and the U═O bond distance.[37] A progressive red shift to the extent of ∼22 cm^{-1} in the symmetric and asymmetric stretching bands, as observed in the spectra b−d of Figure 5, thus reflects on the perturbation of the uranyl ions arising because of their bonding with the framework silicate and resulting thereby in the weakening of the U═O bond.

The IR results of the present study thus reveal that the uranyl groups in U−MCM-48 samples may exist in two distinct environments, one in the framework sites and the other at the terminal sites of the silica wall. These views find support when we compare the IR spectra (b−d) with the spectrum (e) in Figure 5 that represents the IR spectrum of a sample prepared through impregnation route. In the case of IU−MCM-48 we observe the uranyl group band at ∼918 cm^{-1} (Figure 5e) compared to its value of 906 cm^{-1} for U−MCM-48 samples. Also, no band at 835 cm^{-1} is seen in the IU−MCM-48 sample (Figure 5e). We may point out that in a linear uranyl group only two frequencies, due to the asymmetric stretch and the bending mode, should appear in the infrared spectrum.[34] The symmetric stretch band at 860 cm^{-1} is active only when the uranyl group lacks a center of symmetry and exhibits a bent structure. The presence of a weak 835 cm^{-1} band in Figure 5 b, c, and d therefore indicates that at least some of the uranyl groups experience a constrained environment in U−MCM-48 samples. These results may be taken as evidence to suggest that in the samples prepared by impregnation method most of the uranyl groups are bound to terminal silica sites in a linear mode, whereas in hydrothermally synthesized samples a part of them get substituted at framework sites also. Thus, on the basis of the IR, DR UV−Visible, NMR, and XRD data, it can be concluded that uranyl groups in U−MCM-48 samples may exist in two different environments, one in the framework sites (Type 1) and the other at the terminal sites of the silicate wall (Type 2). These two possible modes of binding of uranyl groups in MCM-48 are shown schematically in Figure 6.

Nitrogen Sorption. Figure 7 shows physical adsorption−desorption isotherms of nitrogen for Si−MCM-48 and U−MCM-48 samples, and the corresponding pore size distribution curves are given in Figure 8. All the samples showed isotherms of type IV, having an inflection at around $P/P_0 = 0.25-0.45$, typical of mesoporous materials.[39,40] The samples exhibit complementary textural and framework mesoporosity as evidenced by the presence of two separate well-defined hysteresis loops. One is in the region $P/P_0 = 0.25-0.45$ and depends on the diameter of mesopores, and the other is at $P/P_0 > 0.8$, corresponding to capillary condensation in the interparticle pores.[41] As is well-known, the position of the inflection in $P/P_0 = 0.25-0.45$ region depends on the diameter of the mesopores, and its sharpness

(36) Bell, J. T.; Biggers, R. E. *J. Mol. Spectrosc.* **1965**, *18*, 247.
(37) Nakamoto, K. *Infrared and Raman Spectra of Inorganic and Coordination Compounds*; Wiley: New York, 1978.
(38) Rabinowitch, E.; Belford, R. L. *Spectroscopy and Photochemistry of Uranium Compounds*; Pergamon Press: Oxford, 1964.
(39) Brunauer, S.; Deming, L. S.; Deming, W. E.; Teller, E. *J. Am. Chem. Soc.* **1940**, *62*, 1723.
(40) Sing, K. S. W.; Everett, D. H.; Haul, R. A. W.; Moscou, L.; Pierotti, R. A.; Rouquerol, J.; Siemieniewska, T. *J. Pure Appl. Chem.* **1985**, *57*, 603.
(41) Chen, X.; Huang, L.; Li, Q. *J. Phys. Chem. B* **1997**, *101*, 8460.

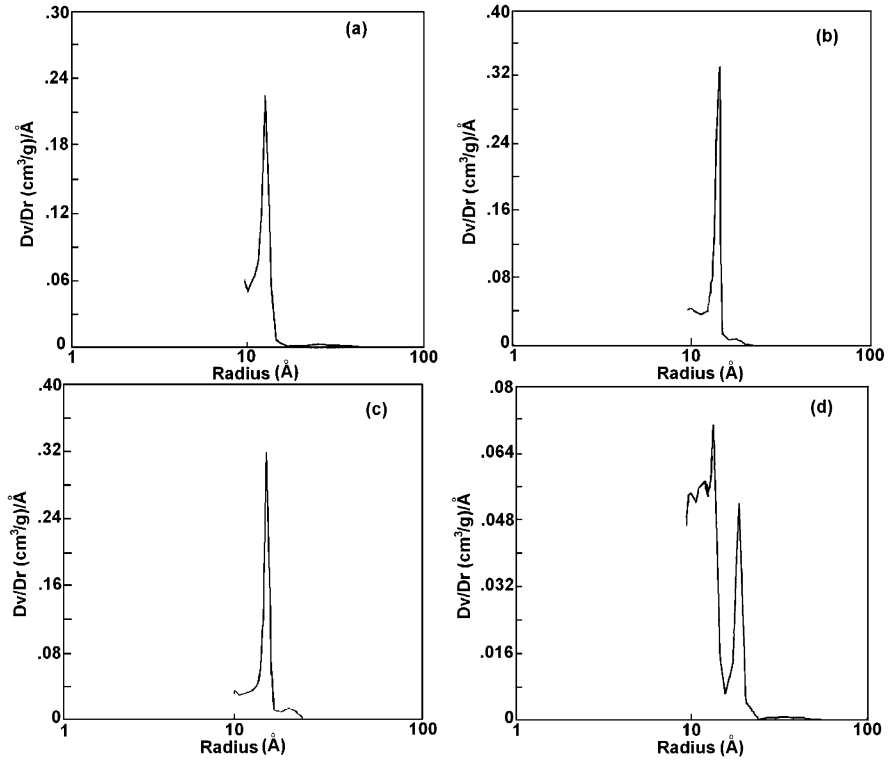

Figure 8. Pore size distribution plots of (a) Si−MCM-48, (b) U−MCM-48A, (c) U−MCM-48B, and (d) U−MCM-48C.

Table 2. Pore Dimensions in the Si−MCM-48, U−MCM-48, and IU−MCM-48 Samples as Calculated from the Desorption Branch of the Nitrogen Sorption Isotherm Using BJH Formula

sample	$BET_{surface\ area}$ ($m^2 \cdot g^{-1}$)	$BJH_{pore\ volume}$ ($cm^3 \cdot g^{-1}$)	$BJH_{pore\ radius}$ (Å)
Si−MCM-48	1414	0.96	14
U−MCM-48A	1190	0.90	16,18
U−MCM-48B	1147	0.86	16, 18
U−MCM-48C	700	0.77	11, 13, 16, 18
IU−MCM-48	800	0.48	11

indicates the uniformity of the pores and the narrow size distribution.[42] A shift in the point of inflection toward higher relative pressure (P/P_0) with increasing uranium content and also a decrease in the sharpness of the inflection point, as observed in Figure 7, are thus indicative of a significant change in the pore size distribution as a result of uranium substitution.

The BET surface area, average pore size distribution as calculated using BJH model, and also the specific pore volumes of Si−MCM-48, U−MCM-48, and IU−MCM-48 samples are presented in Table 2. Whereas Si−MCM-48 sample shows an average pore radius of about 14 Å, the average pore radius in the uranium-containing samples increases to about 16 Å. Also some new pores of about 18 Å radius are seen developing in these samples and their number is found to increase with the increase in the uranium content (Figure 8). The increase in pore size as mentioned above, and also the development of new pores of about 18 Å radius size, in U−MCM-48 samples may be attributed to the larger size of uranyl groups as compared to that of Si^{4+}. Such an increase in pore size has been reported for the incorporation of other metal systems, such as Ce, V, Ti, and Sn, into the silicate framework.[29,43,44] Also, in U−MCM-48C, we observe two additional kind of pores having radius of ∼11 and 13 Å. This may be attributed to blocking of some of the pores by crystallites of α-U_3O_8, formed at high uranium loading. This is in agreement with our XRD results, and the two low intensity peaks observed between the reflections {211} and {220} in Figure 2d can thus be attributed to the filling of some of the pores, leading thereby to their contraction. The pore filling due to impregnation or encapsulation is reported to lead to decrease of d values and hence an increase of 2θ values. This nonuniform pore size distribution in U−MCM-48C is also reflected in the widening of the inflection point (Figure 7d). In addition, a significant decrease in the surface area and the pore volume of this sample can be related to the partial loss of long range ordering, as is also seen in the XRD pattern of Figure 2d.

The observed contraction of some of the pores in U−MCM-48C samples due to dispersion of oxide within the pores finds support in the results obtained for the IU−MCM-48 sample, prepared by impregnation route, where again a similar contraction in pore size radius from 14 to 11 Å is observed due to filling of the pores (Table 2). The results of this study thus clearly indicate that the mode of incorporation of uranium depends on the method of preparation and the amount of uranium loaded. In the samples prepared by hydrothermal synthesis route, a part of uranium occupies the silicate framework positions, which leads to an increase in the pore size and the wall thickness of the material. At the same time, in the sample having higher loading of ∼6%,

(42) Luan, Z.; He, H.; Zhou, W.; Cheng, C. F.; Klinowski, J. *J. Chem. Soc., Faraday Trans.* **1995**, *91*, 2955.

(43) Pak, C.; Haller, G.L. *Microporous Mesoporous Mater.* **2001**, 44−45, 321.

(44) Chaudhari, K.; Das, T. K.; Rajmohanan, P. R.; Lazar, K.; Sivasanker, S.; Chandwadkar, A. J. *J. Catal.* **1999**, *183*, 281.

(45) Alfredsson, V.; Anderson, M. W. *Chem. Mater.* **1996**, *8*, 1141.

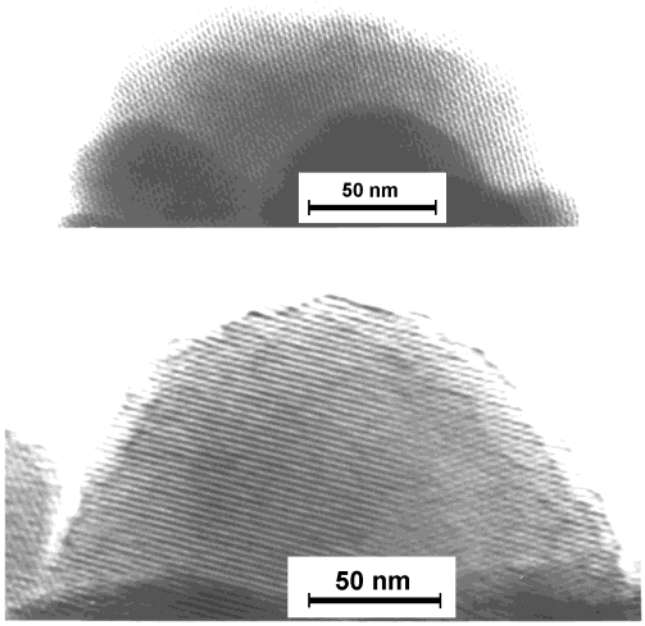

Figure 9. TEM monograph of Si−MCM-48 (a) along [110] direction and (b) along [111] direction.

a small fraction of uranium segregates and disperses as nanocrystallites of U_3O_8 on calcination, resulting thereby in the partial blocking of the pores of MCM-48.

TEM. Low-magnification TEM images showed that the specimen particles comprised sheet-like structures, which were more or less rounded. This appearance is because of the technique used for specimen preparation, wherein the specimen is split into thin sheets along a few preferred crystallographic planes due to the crushing action involved in specimen preparation. HREM images of the pristine specimen were taken along various directions, i.e., [100], [110], and [111] directions. In the [100] direction the pores were found to be arranged in a square grid, and in the [111] and [110] directions the pore arrangements were hexagonal and a distorted hexagon, respectively. The observations along [100] direction were very few in comparison to those along the other two directions. Figure 9a and b show these images for the Si−MCM-48 sample, taken along [110] and [111] directions. These micographs exhibit the presence of a uniform pore structure, and the features in Figure 9 are similar to those reported for this material by other researchers.[23,28,45]

The micrographs a and b of Figure 10 present the typical TEM images of U−MCM-48C taken along [110] and [111] directions, respectively. These pictures reveal no substantial change in the pore arrangement as a result of uranium loading. Minor deformations showing some disordering in the pore structure, are, however, noticeable (see Figure 10a) and may arise due to incorporation of uranium. Such deformation and disordering in the structure are in agreement with the low-angle XRD results on this sample. The presence of dark regions in Figure 10a and b, varying in size from 2 to 5 nm, may be attributed to very uniform and fine dispersion of U_3O_8 crystallites within the host material. As

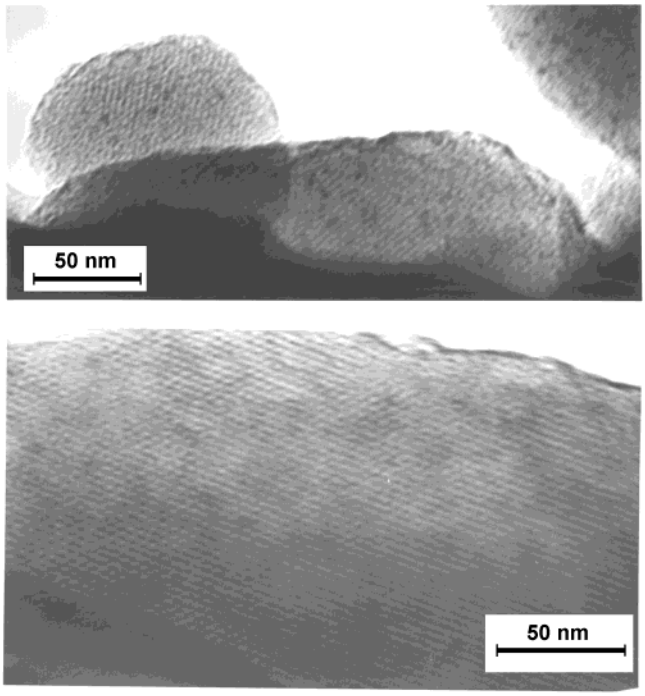

Figure 10. TEM monograph of U−MCM-48C (a) along [110] direction and (b) along [111] direction.

these images are seen more clearly and with a better contrast in the picture taken along {110} direction (Figure 10a), it is likely that the nanocrystallites of U_3O_8 are located in the channels of MCM-48.

Conclusions

To summarize, we have demonstrated in this study a possibility of incorporation of small quantities of uranium in the silicate framework of MCM-48 matrix. The uranium existed in the hexavalent state forming a local uranate type structure and the uranyl groups may bind in two distinct modes, one in the framework sites of silicate matrix and the other at the external surface of the mesoporous walls of MCM-48. In the case of sample with U-loading at around 6 wt %, some of the uranyl groups segregated and gave rise to uniform dispersion of nanosized crystallites of U_3O_8 after calcination. The overall effect is the formation of a multipore mesostructured material, where the uranium at silicate framework sites results in the pores of size larger than that of Si−MCM-48 while the narrower pores are generated due to filling of the mesopores by nanosized U_3O_8 crystallites. It is, however, not possible at this stage to make a quantitative assessment of the above-mentioned uranium moieties, the content of which may vary in a particular sample as a function of U-loading and with the change of synthesis conditions.

Acknowledgment. We thank Dr. J. P. Mittal, Director, Chemistry and Isotope Group, and Dr. S. Banerjee, Director, Materials Group, BARC, for their kind support to this study. We also thank Dr A. K. Tripathi for his help in TEM analysis.

CM030269S